

Supporting Information

H-D-isotope effect of heavy water affecting ligand-mediated nanoparticle formation in SANS and NMR experiments

*Sebastian W. Krauss^a, Mirco Eckardt^a, Johannes Will^b, Erdmann Spiecker^b, Renée Siegel^c, Martin Dulle^d, Ralf Schweins^e, Brian Pauw^f, Jürgen Senker^c, Mirijam Zobel^{*g}*

^a Department of Chemistry, University of Bayreuth, Universitätsstr. 30, 95447 Bayreuth, Germany

^b Institute of Micro- and Nanostructure Research & Center for Nanoanalysis and Electron Microscopy (CENEM), Friedrich-Alexander-Universität Erlangen-Nürnberg, IZNF, Cauerstraße 3, 91058 Erlangen, Germany

^c Inorganic Chemistry III and Northern Bavarian NMR Centre, University of Bayreuth, Universitätsstr. 30, 95447 Bayreuth, Germany

^d JCNS-1/IBI-8: Neutron Scattering and Biological Matter, Forschungszentrum Jülich GmbH, Wilhelm-Johnen-Straße, 52428 Jülich, Germany

^e Institut Laue-Langevin, DS/LSS, 71 Avenue des Martyrs, Grenoble 38000, France

^f Bundesanstalt für Materialforschung und -prüfung (BAM), Unter den Eichen 87, 12205 Berlin, Germany

^g Institute of Crystallography, RWTH Aachen University, Jägerstr. 17-19, 52066 Aachen, Germany

Content

Size comparison with different techniques	2
XRD and PDF data	2
DLS data	5
Particle sizes from DLS and TEM samples for different ageing	5
TEM data	6
Theoretical calculation of <i>pH</i> value during reaction	7
Titration of EDTA complex	8
SAXS and SANS data	9
NMR data	13
UV-vis data	16
References	16

Size comparison with different techniques

Table S1: Diameters of CdS NPs as observed for syntheses in H₂O and D₂O via different characterization techniques for reactant concentrations of 6.25 mM. SAXS, SANS and DLS, analysis is based on spherical shape functions.

	d_{SAXS} (nm) ^a	d_{SANS} (nm)	d_{DLS} (nm) ^c	d_{PDF} (nm)	d_{TEM} (nm) ^d	$d_{\text{TEM, 11d}}$ (nm) ^e
H ₂ O	4.2 ± 0.2	NA ^b	7.6 ± 1.7	3.5	4.1 ± 1.3	4.3 ± 0.7
D ₂ O	5.6 ± 0.2	4.8 ± 2.4	13.7 ± 2.7	2.9	4.4 ± 1.2	5.2 ± 1.0

^a data from BAM with fits in McSAS based on volume-weighted means; ^b For 100 % H₂O, the incoherent scattering is too high that no structural signal can be retrieved from SANS data; ^c volume-squared weighted diameters; ^d mean value of four different syntheses; ^e NPs were stored in dispersed state at room temperature in the respective solvent for 11 days;

XRD and PDF data

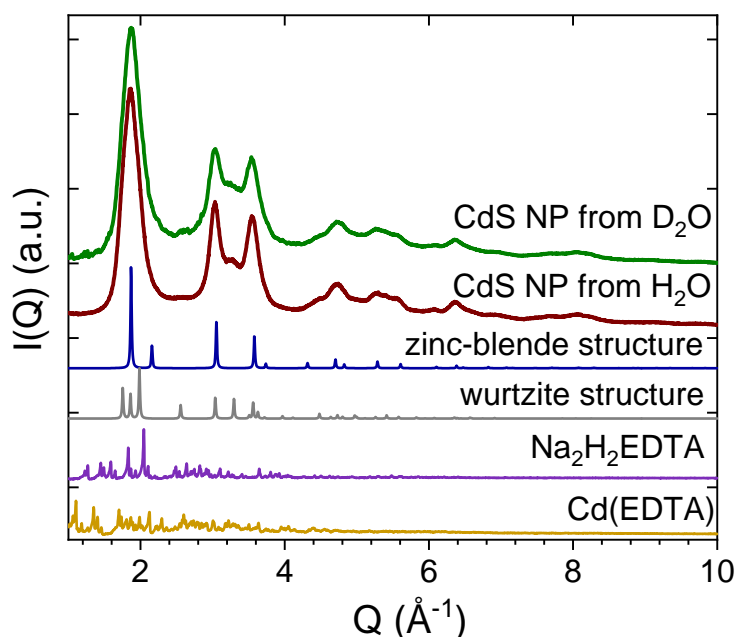


Figure S1: Experimental PXRD pattern of EDTA-stabilized CdS nanoparticles prepared in H₂O and D₂O. Reflexes can be indexed with either the wurtzite or zinc-blende structure. Na₂H₂EDTA and [Cd(EDTA)]²⁻ residuals are visible at small Q-values. Zinc-blende and wurtzite reference pattern are calculated, whereas Na₂H₂EDTA and [Cd(EDTA)]²⁻ reference pattern were recorded by ourselves. The curves are scaled for clarity.

Although CdS NPs powders were washed multiple times with water, the side phase persisted – yet with a very small amount. This XRD data was converted to PDFs using a Q_{max} of 17.5 Å⁻¹. The small phase fraction of Cd-EDTA complexes and pure EDTA seen as side phases in the XRD is so little as to not impact the PDF refinements.

Table S2: Final parameters of the PDF refinements of EDTA-stabilized CdS NPs prepared in H₂O and D₂O. For each solvent, two different samples were prepared and refined (for graphics see Fig. S2).

	CdS _{H2O} , sample 1 (Lab)		CdS _{H2O} , sample 2 (ID31)		CdS _{D2O} , sample 1 (Lab)		CdS _{D2O} , sample 2 (ID31)	
	40 Å	10 Å	40 Å	10 Å	40 Å	10 Å	40 Å	10 Å
r_{\max}								
$a = b$ wurtzite (Å)	4.143	4.135	4.131	4.116	4.146	4.123	4.146	4.147
c wurtzite (Å)	6.774	6.780	6.763	6.766	6.771	6.783	6.771	6.778
$a = b = c$ zinc blende (Å)	5.860	5.872	5.850	5.869	5.857	5.882	5.857	5.848
crystallite size (nm)	3.47	3.47 *	3.53	3.53 *	2.88	2.88 *	2.89	2.89 *
$U_{\text{iso,Cd}}$ (Å ²)	0.028	0.028	0.025	0.024	0.035	0.035	0.035	0.027
$U_{\text{iso,S}}$ (Å ²)	0.034	0.034	0.035	0.038	0.042	0.039	0.042	0.033
stacking fault density (%)	-	40.1 #	-	43.7 #	-	36.1 #	-	38.7 #
R_w	0.15	0.07	0.15	0.09	0.16	0.11	0.16	0.12

* values were inherited from the fit over 40 Å; # values were directly calculated from the phase ratio of wurtzite and zinc-blende.

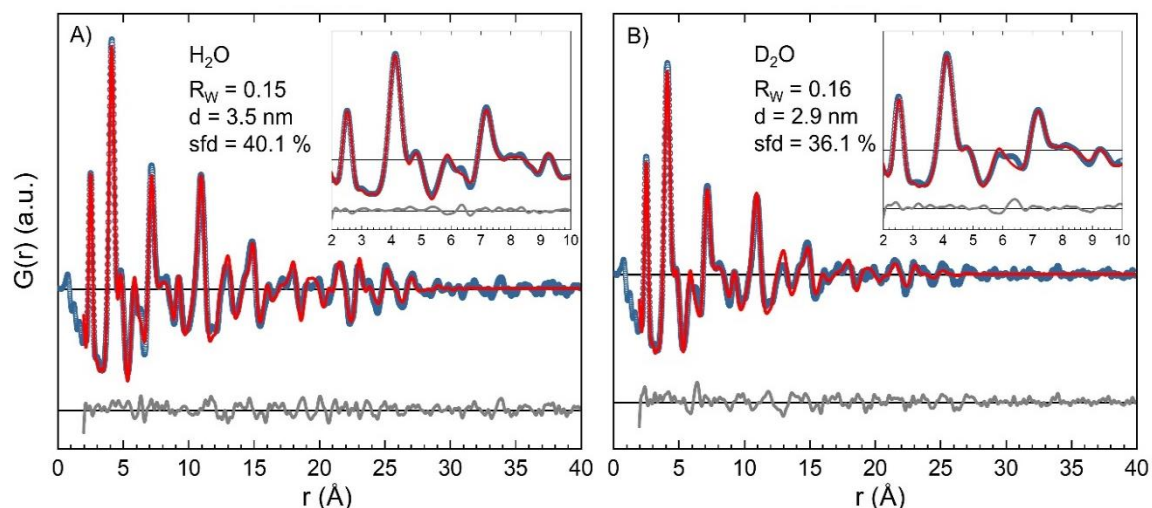


Figure S2: PDF refinements of EDTA-stabilized CdS NP powders⁷ over the range of 2.0 to 40 Å prepared in H₂O (left) and D₂O (right), with the inset zooming into $r = 2.0 - 10$ Å. Refinements were done according to ¹, showing experimental PDFs as blue open circles, model PDFs as red lines and difference curves in grey in offset. This PDF fits are shown exemplarily as for each sample two different samples were prepared and refined. All refinements show good agreement with the experimental data. For values of fit parameters see Table S2.

For the determination of the stacking fault density, we used the model postulated by Yang et al. on 1.3 to 3.6 nm ultrasmall CdSe nanoparticles.¹ We could also fit a hexagonal wurtzite or a cubic zinc-blende crystal structure to the experimental PDF of our CdS NPs. Both represent the data quite well but still

some features remain unfitted. This indicates a mixture of the both faces. The used model takes into account that the wurtzite and zinc-blende structures only deviate in the stacking sequence, A-B and A-B-C, respectively. Thus, the stacking fault density can be expressed by the probability of the third sequence being A (wurtzite) or C (zinc-blende), which can be directly accessed from the ratio of wurtzite in contrast to zinc-blende contribution in a two-phase refinement. Fits of both, CdS NPs powder precipitated from reaction in H₂O and D₂O, were performed on two different samples to prove reproducibility. They resulted in low R_w values of 0.15 and 0.16, respectively, over the r -range of 40 Å. The crystallite size of the D₂O CdS NPs determined from PDF refinement is 0.6 nm smaller than the one of H₂O CdS NPs. Also, U_{iso} values are significantly higher. This indicated distinctively higher disorder in the D₂O CdS NPs, because the overall particle diameter determined from other techniques (TEM, SAXS) is even larger for the D₂O CdS NPs than for the H₂O CdS NPs. The small difference in the stacking fault densities of H₂O and D₂O CdS NPs powders is regarded as not significant.

DLS data

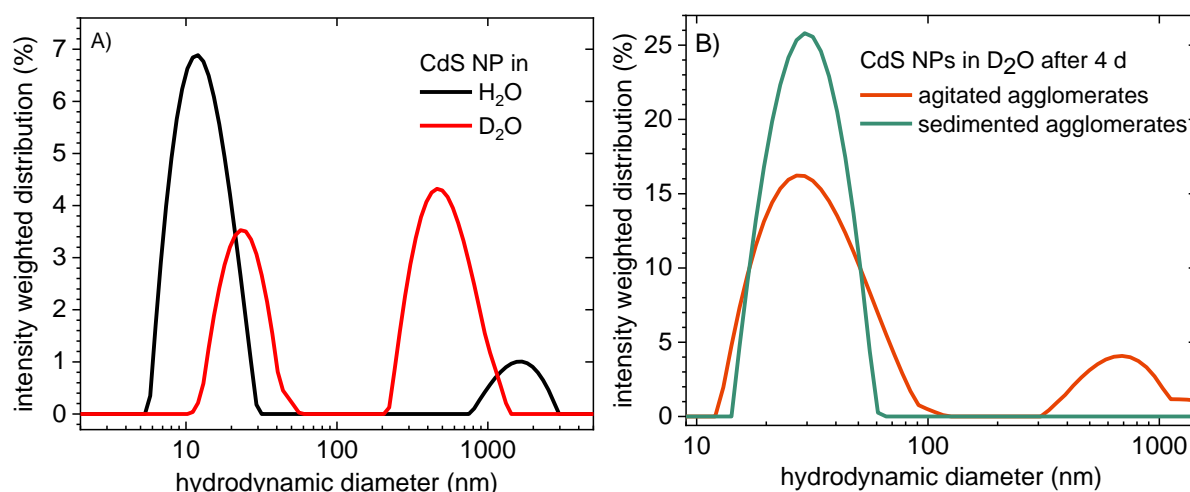


Figure S3: Intensity weighted ($\sim r^6$) size distribution obtained from dynamic light scattering measurements: (A) CdS NPs synthesized in H₂O (black) and D₂O (red) 15 min after the synthesis; (B) sample of CdS NPs in D₂O after storage for 4 d without stirring without measurable aggregates due to sedimentation (green) and detectable aggregates after shaking / agitation of the sample (orange).

Dynamic light scattering measurements were performed to analyse the size of the CdS NPs. Thus the refractive index and absorption coefficient were used for size calculation. Figure S3 a shows the different intensity weighted size distribution of CdS NPs in H₂O and D₂O. Whereas in H₂O two different populations (6 – 12 and > 1000 nm) were detected, in D₂O a third population between 100 and 1000 nm arises. The largest population (> 1000 nm) can be accounted as dust or other dirt particles and the smallest population as the signal from the CdS NPs. The medium population, which is generally visible in D₂O, however, stems from bigger CdS nanoparticles, which can be also seen in SAS analysis. The formation of a larger not-dispersible species is further confirmed by Figure S3 b. Without a steady flow caused by e.g. stirring, this structure settles at the bottom of the vial.

Particle sizes and zeta potentials from DLS and TEM samples for different ageing

Table S3: Summary of all measured single datapoints for the size and ζ -potential determination of the CdS NPs. Indexes specify the age of samples. No index represents as-synthesized samples with measurements within few hours after synthesis.

	d_{TEM} (nm) ^a	$d_{\text{TEM, 11 d}}$ (nm)	$d_{\text{TEM, 22 d}}$ (nm)	$d_{\text{TEM, 60 d}}$ (nm)	d_{PDF} (nm)	d_{DLS} (nm)	ζ -potential (mV)
H₂O	4.3 ± 1.1	4.5 ± 1.0		5.5 ± 1.3	3.5	8.2 ± 2.0	-19.2 ± 0.9
	4.3 ± 1.2				3.5		
	4.3 ± 1.4		4.5 ± 1.0			7.2 ± 1.9	-13.7 ± 0.8
	3.0 ± 0.9	4.8 ± 2.1				7.5 ± 1.4	-25.6 ± 1.2
D₂O	4.2 ± 1.0	5.8 ± 1.2		4.6 ± 0.9	2.9	6.0 ± 1.6	-10.9 ± 1.1
	5.1 ± 1.3				2.9		
	4.0 ± 1.6		5.0 ± 1.1			13.3 ± 2.5	-15.3 ± 1.1
	4.2 ± 0.9	5.0 ± 1.3				21.7 ± 2.8	-31.0 ± 1.5

TEM data: HR-STEM data (top) and particle size analysis (bottom)

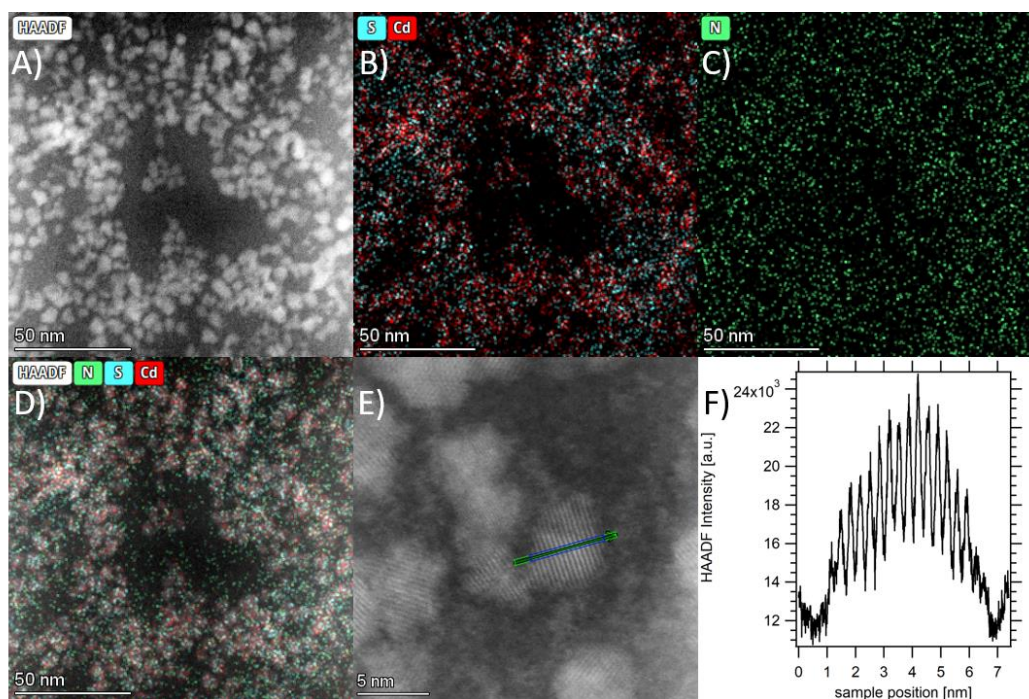


Figure S4: A-D) STEM-EDX maps of dried CdS NPs, which were freshly prepared in H₂O. The bright contrast in HAADF imaging nicely correlates with the Cd and S signal. Moreover, the N signal is enhanced in regions next to CdS NPs. E) HRSTEM image of CdS NPs. A line-cut perpendicular to the lattice fringes indicated in E) is displayed in F). The extracted lattice parameter of 3.37 Å fits to the (111) lattice spacing in the zinc blende structure (3.38 Å as refined via PDF in Table S2). The cloudy contrast surrounding the CdS NPs stem from organic ligands, revealing their abundance in particular close to NPs.

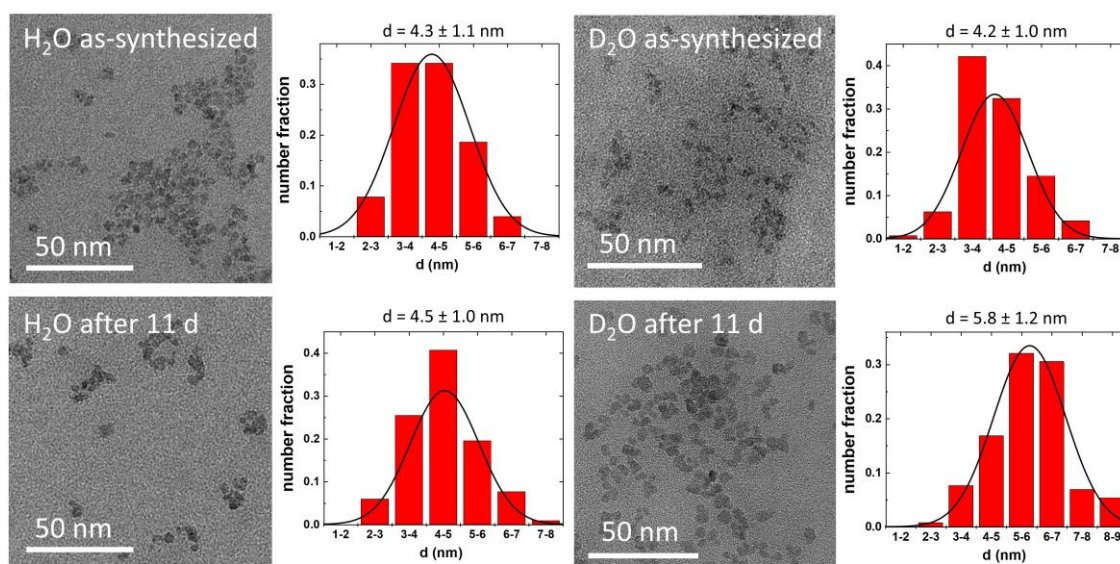


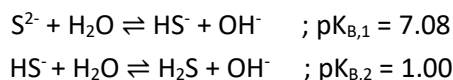
Figure S5: TEM images of EDTA stabilized CdS NPs prepared in H₂O (left) and D₂O (right) with the corresponding histograms and Gaussian fits of the size distribution. The samples were prepared directly after the synthesis (upper line) and after storage as aqueous suspension for 11 days (lower line).

The TEM study of the colloidal stability of the CdS NPs over 11 days shows a significant growth of the particles in D₂O from 4.2 ± 1.0 to 5.8 ± 1.2, whereas in H₂O the particle size stays the same in the margin of error.

Theoretical calculation of pH

The pH value for different reaction times is estimated as follows based on molar turnover or equilibrium constants, and compared to experimentally observed pH values. Experiments and calculations were done based on aqueous 6.25 mM stock solutions of i) $\text{Na}_2\text{S} \cdot 9 \text{H}_2\text{O}$ and ii) 1 : 1 mixture of $\text{CdCl}_2 \cdot 2.5 \text{H}_2\text{O}$ and $\text{Na}_2\text{H}_2\text{EDTA} \cdot 2 \text{H}_2\text{O}$.

The stock solution of Na_2S shows a pH of ca. 11, since $\text{Na}_2\text{S} \rightarrow 2 \text{Na}^+ + \text{S}^{2-}$ with subsequent reactions

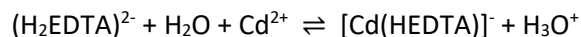


The $\text{Na}_2\text{H}_2\text{EDTA}$ solution has an experimental pH value of 4, since $\text{H}_2\text{EDTA}^{2-}$ dissociates further with two equilibria (EDTA in total features 4 such equilibria with $\text{p}K_1 = 1.99$, $\text{p}K_2 = 2.7$, $\text{p}K_3 = 6.2$ and $\text{p}K_4 = 9.8$; values from ²):



According to literature, Cd-EDTA complexes at $\text{pH} < 3$ can be found in solution in a deprotonated form $[\text{Cd}(\text{EDTA})]^{2-}$ or monoprotonated form $[\text{Cd}(\text{HEDTA})]^-$, see Fig. 2 in ³.

Calculations show that our experimentally observed pH value of 2.2 upon the addition of the aqueous $\text{CdCl}_2 \cdot 2.5 \text{H}_2\text{O}$ to the aqueous $\text{Na}_2\text{H}_2\text{EDTA}$ solution can be reasoned by an average cleavage of one proton:



Therefore, the amount of oxonium ions equals the amount of introduced Cd^{2+} ions.

$$\text{pH}_{\text{theo}} = -\log(6.25\text{mM}/1\text{M}) = 2.2$$

The calculated pH then equals the measured pH of 2.21.

Upon the mixing of aqueous Na_2S with CdCl_2 -EDTA stock solution, OH^- reacts with H^+ and thus an increase in pH occurs due to this neutralization. This increase in pH from 2.21 to 2.46 happens instantaneously so that our monitored start value of the pH monitoring in Fig. S6 represents the pH after this neutralization.

Subsequent increases in pH values stem from CdS particle growth and new chemical equilibria of various Cd-EDTA complex species of varying protonation degree are reached over time.

Up to 1 min (Fig. S7) most of the particle formation takes places and the pH increases in H_2O from 2.46 to 2.59 (respectively from 2.51 to 2.63 in D_2O). To achieve this increase in the titration for the pure Cd-EDTA complex, 0.33 equivalents or 2.1 mM NaOH have to be added. Therefore, approximately 2.1 mM of oxonium ions in H_2O and 1.2 mM oxonium ions in D_2O are consumed. For H_2O this consumption of about 2.1 mM H_3O^+ ions roughly correspond to the value of 2.5 mM Cd^{2+} ions which react out of the 6.25 mM initial CdCl_2 based on the approximate yield of CdS of 40%. Since on average, we calculated the pH value to match $[\text{Cd}(\text{HEDTA})]^-$ complexes, these values agree quite well and it is likely that in a quick precipitation $2.1/2.5 = 84\%$ of the overall yield are achieved fast with a subsequent reaction of

further complexes until the reaction finally stops. During the second increase in pH for times > 10 min, another 0.4 mM oxonium ions are consumed in H₂O.

For D₂O the initial reaction consumes 1.2 mM oxonium ions, but another 1.3 mM are consumed for times > 10 min (also estimated by titration of Cd-EDTA complex). This further underpins our idea, that in D₂O a secondary growth process by inclusion of further complexes takes place over days.

Titration of Cd-EDTA complex

The Cd-EDTA complex was titrated in H₂O and D₂O against 0.1 M NaOH in H₂O or D₂O. The corresponding measured pH values are shown in Fig. S5.

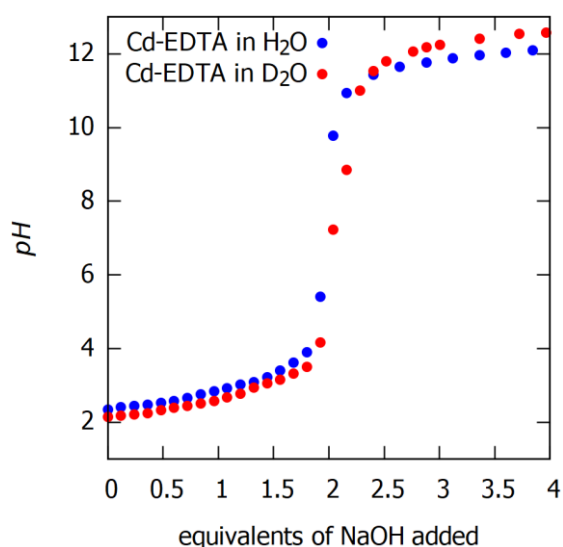


Figure S6: Titration of Cd-EDTA complex with NaOH in H₂O (blue) and D₂O (red)

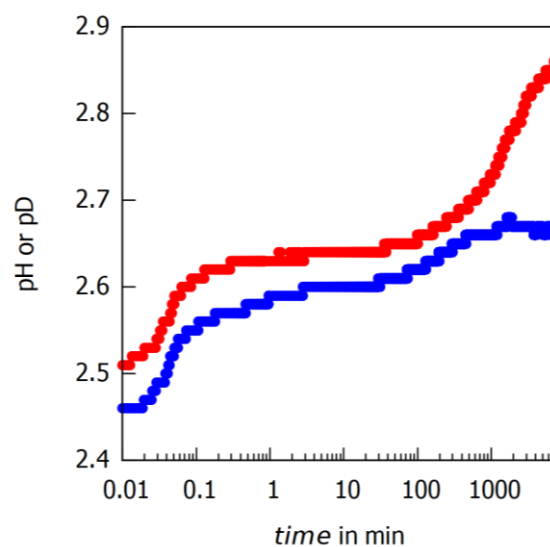


Figure S7: Evolution of pH during CdS NP formation in H₂O and D₂O; In contrast to Fig. 6, all measured data points are plotted.

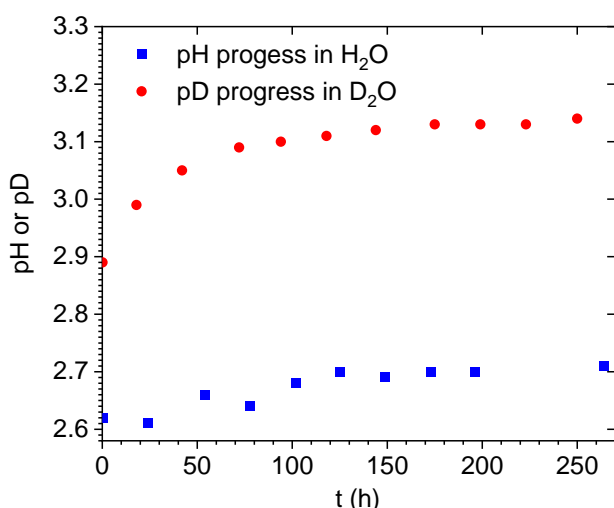


Figure S8: Long-term pH/pD study of CdS NPs synthesized in H₂O (blue) and D₂O (red). The starting pD for CdS NPs in D₂O is slightly shifted in comparison to Figure S7, but approves the trend and shows that both, pH and pD, approach a plateau.

SAXS and SANS data

Data of SAXS and SANS refinements in SasView

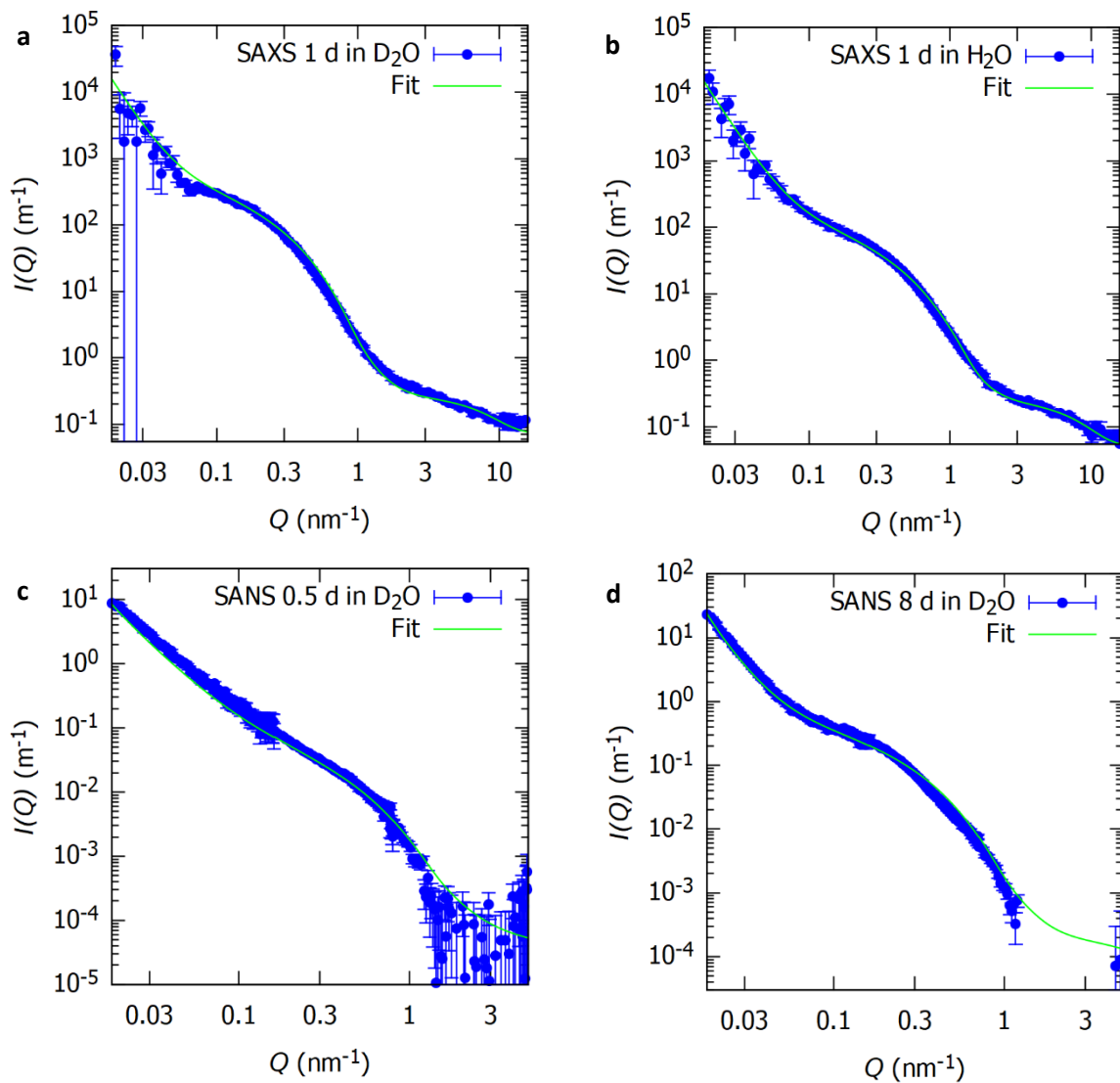


Figure S9: Refinement of SAXS and SANS data for CdS nanoparticle suspensions in D_2O (panel a,c,d) and H_2O (b), for different times (in days) after NP synthesis. Modelling of data was carried out in SasView.

SAXS Fitparameter

scattering length density	3.41e-05 /Å ²
scattering length density solvent	9.47e-06 /Å ²
background	0.05 cm ⁻¹
scale 1	4 e09
radius 1	16.5 nm
distribution of radius 1	0.5 PD
volume fraction 1	0.19
perturbance 1	0.05
stickiness 1	0.108
scale 2	51.9 e09
radius 2	1.5 nm
distribution of radius 2	0.5 PD
scale 3	15.3 e09
volume fraction 3	0.0686
radius 3	0.113 nm
fractal dimension 3	2.89
length 3	7140 Å

Table S4: Parameters that have been used to Fit the graph in Fig. 5

McSAS refinements of SAXS data (BAM)

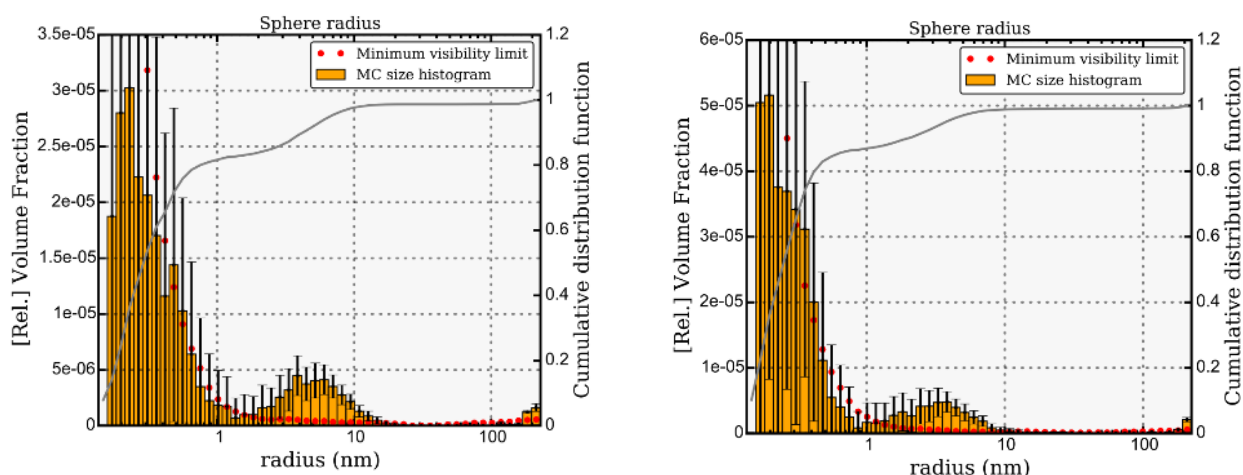


Figure S10: Absolute volume fraction and corresponding cumulative distribution function of CdS NPs in D₂O (left) in H₂O (right) as determined with McSAS refinement from SAXS patterns of (MAUS, BAM).

Modelling of SAXS data with McSAS, assuming spherical scatterers, converging to a chi-squared of 1. The data uncertainties at the extrema are high due to the large background scattering of the dispersant (H₂O, D₂O) at high Q , and the instrumental background at low Q . A small, sub-nm population is evident, as well as the particle population between 1-20 nm, and finally a small amount of agglomerates is visible towards the upper extreme. The volume fraction and population statistics of the particle population in radius can be extracted to be:

	D ₂ O	H ₂ O
Range, volume-weighted	1.500e-09 to 1.000e-07	1.500e-09 to 1.000e-07
Total volume fraction of particles	3.872e-05 ± 1.607e-06	4.001e-05 ± 2.420e-06
Mean (m), volume-weighted mean	5.605e-09 ± 2.013e-10	4.178e-09 ± 1.662e-10
Variance (m ²), square root of the distribution width sigma		1.317e-17 ± 3.692e-18

Table S5: Results of McSAS fit parameters

The McSAS refinement reveals a lot of unreacted CdCl₂ salt / Cd-EDTA complexes respectively. Beyond this, there is a population of CdS particles with a mean radius of about 5.6 nm for D₂O, and a volume fraction of 3.9 e-5 (= 0.174 mg/ml assuming cubic CdS). In H₂O, this CdS NP population has a smaller population mean of about 4.2 nm, and a slightly higher volume fraction of 4e-5 (=0.18 mg/ml). We do observe, both for H₂O and D₂O a fraction of larger particles, which based on the high data uncertainty can only be said to be in the range of 100 nm to 1 μm.

Contrast match series of SANS data

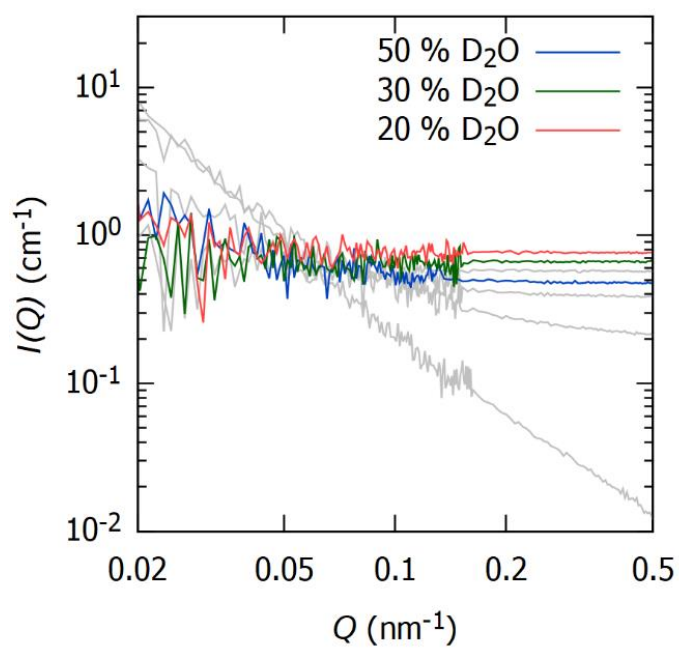


Figure S11: SANS contrast match series showing the solvent mixtures D_2O - H_2O with 20, 30 and 50 % D_2O in color (red, green, blue respectively), while datasets already plotted in Fig. 5b are added for comparison in grey.

Further NMR data

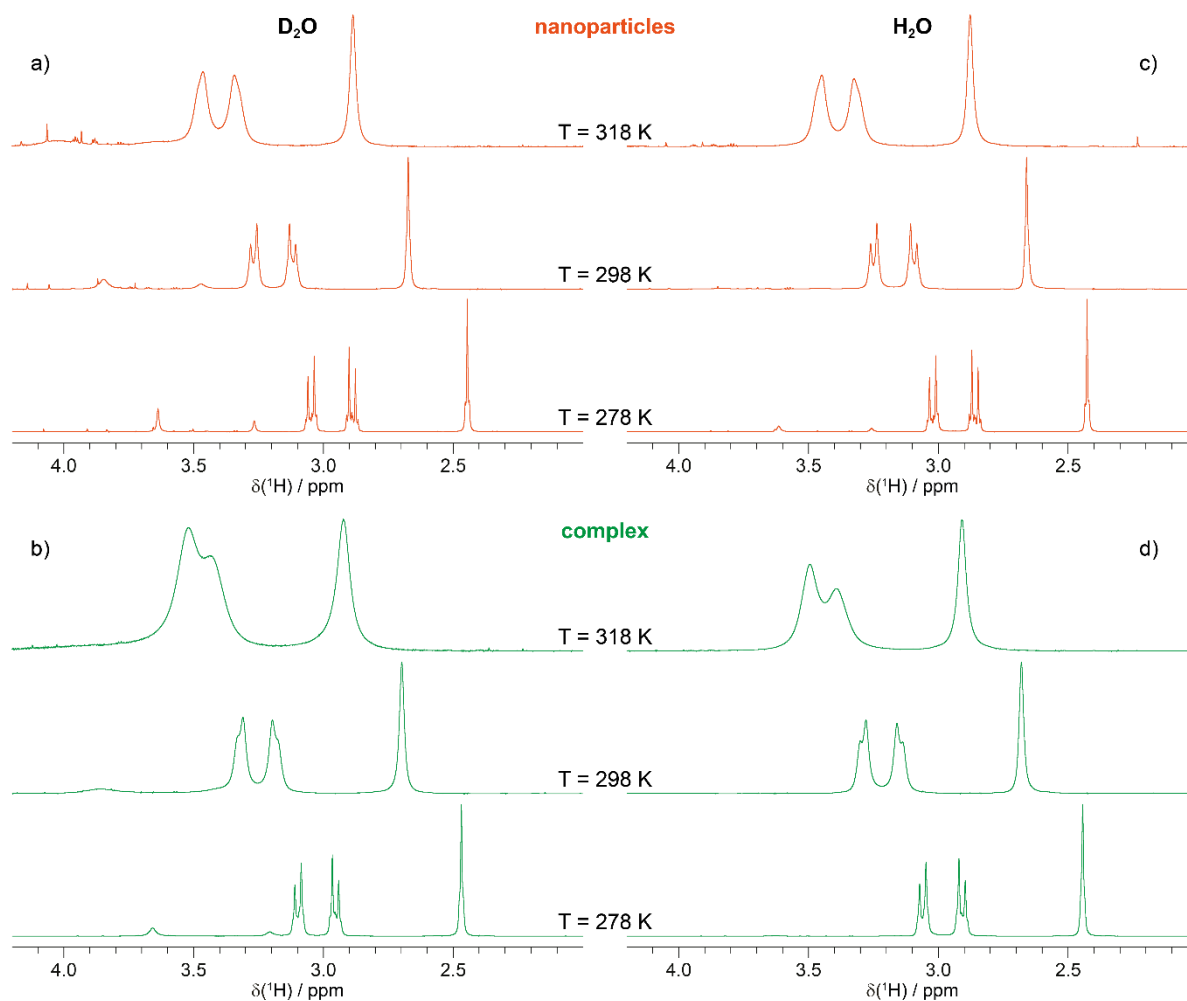


Figure S12: ¹H liquid-state NMR spectra of a) CdS NPs and b) [Cd(EDTA)]²⁻ complex in D₂O, and c) CdS NPs and d) [Cd(EDTA)]²⁻ complex in H₂O at different temperatures (indicated in the figures).

For a spherical nanoparticle with a diameter of about 6 nm, the Stokes-Einstein relation, $\tau_c =$

$$\frac{4\pi\eta r^3}{3k_B T},$$

gives a correlation time τ_c of about $3.10 \cdot 10^{-8}$ s

In the slow-exchange regime, i.e. extreme narrowing limit where $\omega\tau_c \ll 1$, we have, in the case of intramolecular dipolar interaction:

$$\frac{1}{T_1} = \frac{1}{T_2} = 2 \cdot \left(\frac{\mu_0}{4\pi}\right)^2 \gamma_H^2 \cdot \hbar^2 \cdot I(I+1) \cdot \frac{1}{r_{HH}^6} \cdot \tau_c$$

With a distance r_{HH} of about 1.5 Å (H-H distance of a CH₂ group), this gives a T₂ relaxation time of $4.4 \cdot 10^{-4}$ s corresponding to a peak full width at half maximum of 4.5 kHz. This latter value is too broad for the nanoparticles to be visible in the liquid-state NMR spectra.

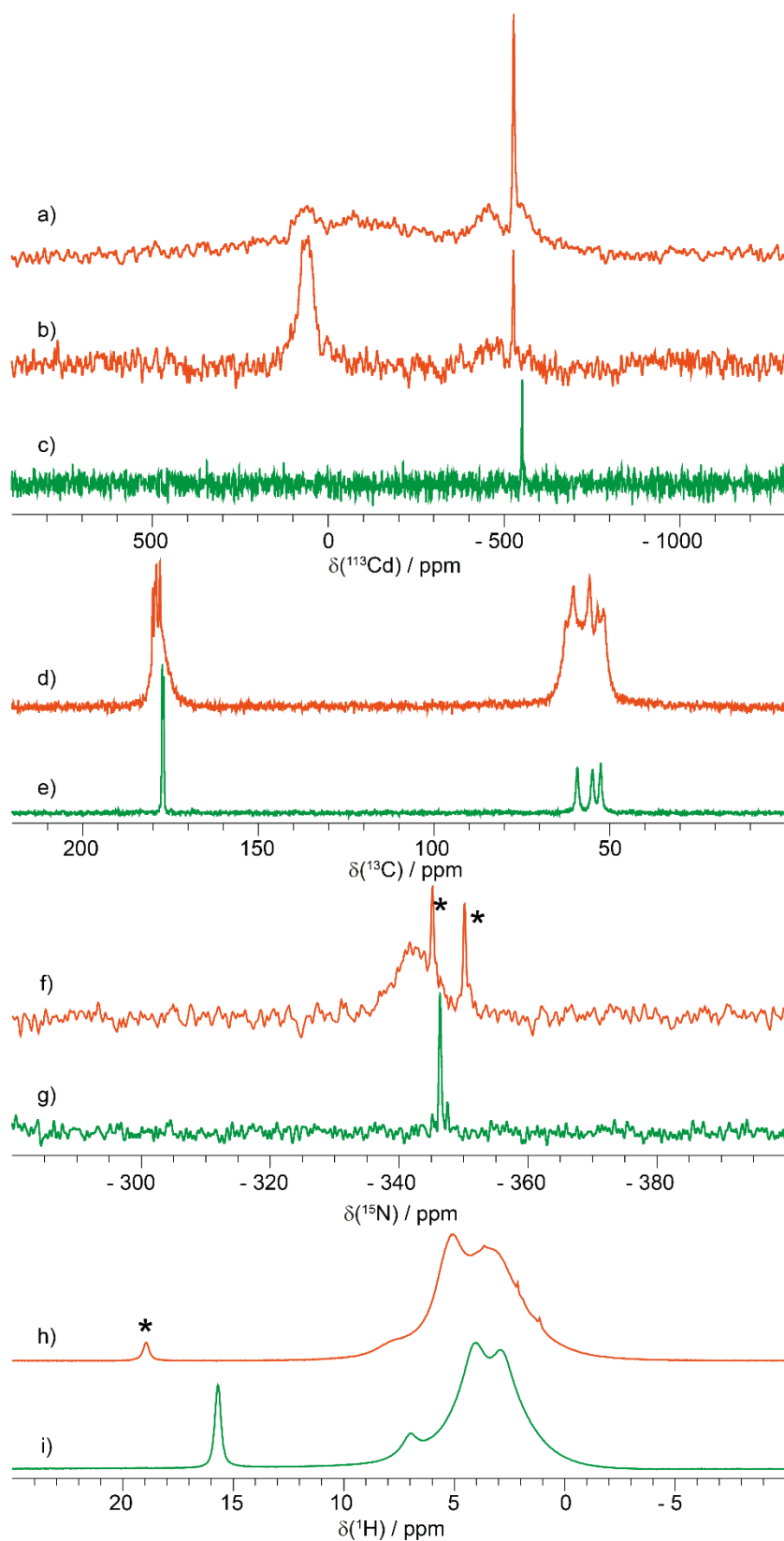


Figure S13: a). ^{113}Cd (a, b, c), ^{13}C (d, e), ^{15}N (f, g) and ^1H (h, i) solid-state MAS NMR spectra of CdS-NPs (orange: a, b, d, f, h) and crystalline $[\text{Cd}(\text{D}_2\text{EDTA})(\text{D}_2\text{O})]\cdot 2\text{D}_2\text{O}$ (green: c, e, g, i) prepared using D_2O . While the spectra displayed in (b, h, i) were recorded with single-pulse excitation, the spectra (a, c, d, e, f, g) were measured using cross-polarization. * indicate impurities from some other EDTA complexes (e.g. $[\text{Na}_2\text{H}_2\text{EDTA}]$) and/or free EDTA.

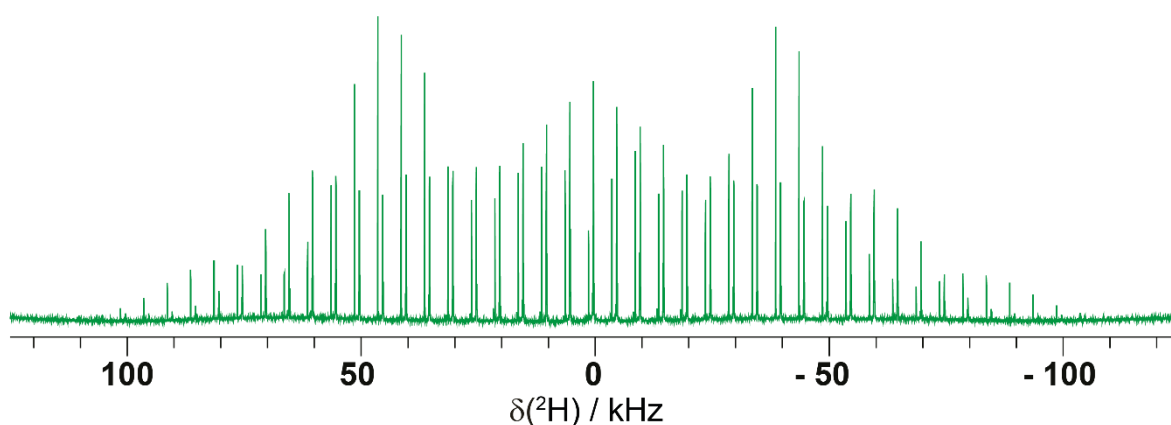


Figure S14: ^2H solid-state MAS NMR spectra crystalline $[\text{Cd}(\text{D}_2\text{EDTA})(\text{D}_2\text{O})]\cdot 2\text{D}_2\text{O}$ complex prepared using D_2O . The two main resonances at about 16 and 4.8 ppm are assigned to the deuterium on the carboxylic acid and water having, respectively, quadrupolar coupling constant of about 135 and 100 kHz with quadrupolar asymmetry of 0.1 and 1. The relatively small quadrupolar interaction of the water is explained by the most probable dynamic of the D_2O . The relative intensities of 1 and 3 for the resonances of the carboxylic acid and of water, respectively, perfectly fits with the assignment and the expected structure which has three different water (one bound to Cd and two crystalline water).

UV-vis data

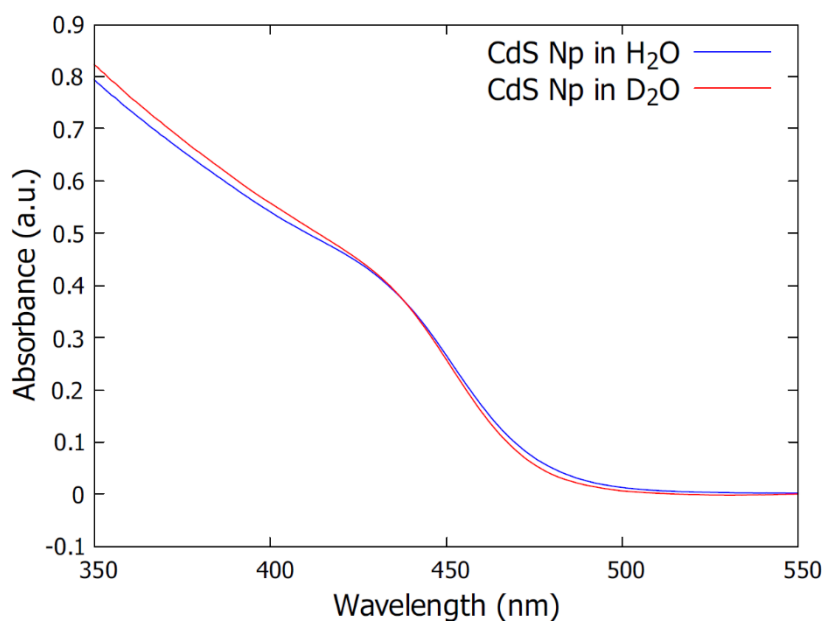


Figure S15: With an exciton bohr radius in CdS of 5.8 nm, there is quantum confinement with crystallite sizes below 5 - 6nm [4]. The absorption profile in H₂O and D₂O is similar. The absorption edge is around ~435 nm and therefore it is strongly blue shifted compared to the bulk form of CdS, where it would be at 510 nm. The synthesised nanoparticles are hence in the quantum dot regime. Over the absorption edge, the H₂O data is slightly red-shifted compared to the D₂O data. This confirms the observations made with PDF, that the crystalline domain size in the CdS nanoparticles in H₂O is larger than in D₂O.

References

- ¹ Yang, X.; Masadeh, A. S.; McBride, J. R.; Bozin, E. S.; Rosenthal, S. J.; Billinge, S. J. L. *Phys Chem Chem Phys* **2013**, *15*, 8480-8486.
- ² Kula, R. J.; Reed, G. H. *Anal. Chem.* **1966**, *38*.
- ³ van Leeuwen, H. P.; Town, R. M. *Environ. Sci. Technol.* **2009**, *43*, 1, 88–93.
- ⁴ Yadav, R. S.; Mishra, P.; Mishra, R.; Kumar, M.; Pandey, A. C. *Ultrasonics sonochemistry*, **2010** *17*(1), 116-122